Entropy production and wave packet dynamics in the Fock space of closed chaotic many-body systems

V. V. Flambaum[1,*] and F. M. Izrailev[2]
[1]*School of Physics, University of New South Wales, Sydney 2052, Australia*
[2]*Instituto de Física, Universidad Autónoma de Puebla, Apartado Postal J-48, Puebla 72570, Mexico*
(Received 22 March 2001; published 29 August 2001)

Highly excited many-particle states in quantum systems such as nuclei, atoms, quantum dots, spin systems, quantum computers, etc., can be considered as ''chaotic'' superpositions of mean-field basis states (Slater determinants, products of spin or qubit states). This is due to a very high level density of many-body states that are easily mixed by a residual interaction between particles (quasiparticles). For such systems, we have derived simple analytical expressions for the time dependence of the energy width of wave packets, as well as for the entropy, number of principal basis components, and inverse participation ratio, and tested them in numerical experiments. It is shown that the energy width $\Delta(t)$ increases linearly and very quickly saturates. The entropy of a system increases quadratically, $S(t)\sim t^2$, at small times, and afterward can grow linearly, $S(t)\sim t$, before saturation. Correspondingly, the number of principal components determined by the entropy $N_{pc}\sim\exp[S(t)]$ or by the inverse participation ratio increases exponentially fast before saturation. These results are explained in terms of a cascade model which describes the flow of excitation in the Fock space of basis components. Finally, the striking phenomenon of damped oscillations in the Fock space at the transition to equilibrium is discussed.

DOI: 10.1103/PhysRevE.64.036220 PACS number(s): 05.45.Mt, 03.67.Lx, 24.10.Cn

I. INTRODUCTION

Highly excited many-particle states in many-body systems quite often can be presented as ''chaotic'' superpositions of shell-model basis states; see recent calculations for complex atoms [1], multicharged ions [2], nuclei [3], and spin systems [4,5]. The origin of this phenomenon relates to a very high density of many-particle energy levels, which increases drastically with increase of energy. Indeed, the number N of combinations in the distribution of n particles (or quasiparticles) over m ''orbitals'' (single-particle states) is exponentially large [$N\sim m!/n!(m-n)!$ in a Fermi system]. Therefore, the spacing D between many-body levels is exponentially small and a ''residual'' interaction V between the particles can mix a huge number of the basis states of the mean field H_0 (Slater determinants) when forming exact eigenstates of the total Hamiltonian $H=H_0+V$.

The onset of chaos for highly excited states, as well as for many-particle spectra, has recently been studied in great detail in terms of the two-body random interaction (TBRI) model, which was invented about three decades ago [6]. In this model all *two-body* matrix elements are assumed to be independent and random variables, and therefore all dynamical correlations are neglected. Thus, the TBRI model is essentially the random matrix model; however, it differs from standard random matrix models where the two-body nature of the interaction is not taken into account (see, e.g., [7–12]).

One of the important results obtained recently [13] in the framework of this model is the Anderson-like transition that occurs in the Fock space determined by many-particle states of H_0 (see also [14]). The critical value V_{cr} for this transition is determined by the density of states $\rho_f=d_f^{-1}$ of those basis states that are directly coupled by a two-body interaction. When the interaction is very weak, $V_0\ll d_f$, exact eigenstates are δ-like functions in the unperturbed basis, with a very small admixture of other components which can be found by the standard perturbation theory. With an increase of the interaction, the number of principal components N_{pc} increases and can be very large, $N_{pc}\gg 1$. However, if the interaction is still not too strong, $\pi^{-2}\sqrt{d_f D}\ll V_0\leqslant d_f$ [8] , the eigenstates are sparse, with extremely large fluctuations of components. In order to have ergodic eigenstates that fill some energy range (see below), one needs to have a sufficiently large perturbation $V_0\gg d_f$ (for a large number of particles this transition is sharp and, in fact, one needs the weaker condition $V_0\geqslant d_f$).

Above the threshold of chaos $V_0\geqslant d_f$, the number of principal basis components in an eigenstate can be estimated as $N_{pc}\sim\Gamma/D$ where Γ is the spreading width of the *strength function*. In such chaotic eigenstates any external weak perturbation is exponentially enhanced. The enhancement factor can be estimated as $\sqrt{N_{pc}}\propto 1/\sqrt{D}$; see, e.g., [15] and references therein. This huge enhancement has been observed in numerous experiments when studying parity violation effects in compound nuclei (see, for example, the review [16]).

In recent work [17,18] the theory of many-body chaos has been extended to quantum computers. Since in this case the density of energy levels is extremely high, it is often impossible to resolve particular many-body levels. This happens for the injection of an electron into a many-electron quantum dot, for the capture of an energetic particle by a nucleus or atom, or for different models of quantum computer with a large number of interacting qubits (spins). In this case the approach based on the study of stationary chaotic eigenstates turns out to be inadequate, and one should consider the time evolution of the wave function and entropy [18].

*Email address: flambaum@newt.phys.unsw.edu.au

In contrast to the study of spectra and eigenstates, analysis of the evolution of wave packets in random matrix models is based mainly on numerical results. First, one should mention the numerical study [19] of band random matrices that describe quasi-one-dimensional disordered models with a finite number of channels. Recently, attention has been paid to the so-called Wigner band random model (WBRM) [20], which is used in the study of generic properties of strength functions in dependence on the strength of the interaction [21,22]. In particular, in Refs. [23,24] the problem of the quantum-classical correspondence for the time evolution of wave packets was under close study. We note that the WBRM serves as a convenient random matrix model for different quantum systems, and in many aspects can be compared with the TBRI model [25].

In this paper we study generic properties of the evolution of wave packets in the energy shell, paying most attention to the time dependence of the entropy, the width of the packets, and the inverse participation ratio. We derive analytical estimates for these quantities and check our predictions numerically using the TBRI and WBR models.

II. TIME EVOLUTION OF CHAOTIC MANY-BODY STATES

Exact (''compound'') eigenstates $|k\rangle$ of a many-body Hamiltonian $H=H_0+V$ can be expressed in terms of simple shell-model basis states $|f\rangle$ (eigenstates of H_0), or by products of qubits in the model of a quantum computer:

$$|k\rangle=\sum_f C_f^{(k)}|f\rangle; \quad |f\rangle=a_{f_1}^{\dagger},\ldots,a_{f_n}^{\dagger}|\text{''vacuum''}\rangle. \quad (1)$$

Here $a_s^{\dagger}$ are creation or spin-raising operators (in the latter case, the ground state $|\text{vacuum}\rangle$ corresponds to the situation with all spins down), and $C_f^{(k)}$ are components of compound eigenstates $|k\rangle$ formed by the residual interaction V.

In what follows, we consider the time evolution of the system for the case when the compound eigenstates are *chaotic*. By this term we mean that the number of principal components is very large, $\sqrt{N_{pc}}\gg 1$, and the components $C_f^{(k)}$ can be treated as uncorrelated amplitudes with a Gaussian distribution around their mean values (see details in [8]). Let us assume that initially $(t=0)$ the system is in a specific basis state $|0\rangle$ (with certain orbitals occupied, or, in the case of a quantum computer, when the state with certain spins ''up'' is prepared). This state can be presented as a sum over exact eigenstates of the total Hamiltonian H:

$$|0\rangle=\sum_k C_0^{(k)}|k\rangle. \quad (2)$$

Then the time-dependent wave function reads as

$$\Psi(t)=\sum_{k,f} C_0^{(k)}C_f^{(k)}|f\rangle\exp(-iE^{(k)}t). \quad (3)$$

Here the sum is taken over the compound states k and basis states f, and we set $\hbar=1$.

The probability $W_0=|A_0|^2=|\langle 0|\Psi(t)\rangle|^2$ of finding the system in the initial state is determined by the amplitude

$$A_0=\langle 0|\exp(-iHt)|0\rangle=\sum_k |C_0^{(k)}|^2\exp(-iE^{(k)}t)$$

$$\simeq\int dE\,P_0(E)\exp(-iEt). \quad (4)$$

Here we replaced the summation over a large number of eigenstates by an integration over their energies $E\equiv E^{(k)}$, and introduced the *strength function* (SF) $P_0(E)$ which is also known in the literature as the *local spectral density of states* (LDOS):

$$P_0(E)\equiv\overline{|C_0^{(k)}|^2}\rho(E), \quad (5)$$

with $\rho(E)$ as the density of exact eigenstates.

As one can see, the probability W_0 is entirely determined by the strength function (5). It is well known that in many applications this function has the Breit-Wigner (BW) form with a full width at half maximum (FWHM) $\Gamma_0=2\pi\rho H_f^2$. In our case $\rho=\rho_f$ is the density of directly coupled basis states and $H_f^2=\overline{|H_{0f}|^2}$ is the variance of the nonzero off-diagonal elements of H, defined by the residual interaction V. One should recall that in real situations the second moment Δ_E^2 of the SF is always finite due to the finite range of interaction in the energy representation. Therefore, the Breit-Wigner form of the SF can occur for a finite energy range only, determined by the energy width of the interaction.

However, it was recently shown (see, e.g., [8,11] and references therein) that if Γ_0 defined by the above expression is of the order of (or larger than) the mean-square-root width Δ_E of the SF itself, the form of the SF in the TBRI model is very close to Gaussian. Strong deviations of the SF from the BW dependence have been observed numerically when studying the structure of the SF and eigenfunctions of the Ce atom [1]. Also, numerical data [3] have revealed that the form of the SF in nuclear shell models is much closer to Gaussian rather than to the BW form. This results from the fact that the three orbitals s, $d_{3/2}$, and $d_{5/2}$ included in nuclear shell-model calculation [3] have close mean-field energies and the residual interaction V plays the dominant role in the Hamiltonian matrix.

Recent analytical results [11] for the TBRI model allow a description of the whole transition for the SF from the BW regime to that of the Gaussian. This model is characterized by two-body random matrix elements which determine the residual interaction V between n Fermi particles occupying m orbitals (single-particle states); see details and references, for example, in [8,25]. It was shown that in the general case the SF is given by the following approximate expression [26,11]:

$$P_0(E)=\frac{1}{2\pi}\frac{\Gamma(E)}{[E_0+\delta_0(E)-E]^2+\Gamma^2(E)/4}, \quad (6)$$

$$\Gamma(E)\simeq 2\pi\overline{|H_{0f}|^2}\rho_f(E). \quad (7)$$

One can see that the general expression (6) is of the Breit-Wigner form, but with $\Gamma(E)$ as some function of the total energy E. Here $\delta_0(E)$ is the correction to the unperturbed energy level E_0 due to the residual interaction V, and $\rho_f(E)$ is the density of those basis states $|f\rangle$ that are directly coupled by the interaction H_{0f} with the initial state $|0\rangle$. It was shown [11] that for the TBRI model the function $\Gamma(E)$ has the Gaussian form with a variance that depends on the model parameters. In the case of a relatively small (but nonperturbative) interaction, $\Gamma_0=2\pi\rho_f H_f^2\ll\Delta_E$, the function $\Gamma(E)$ is very broad (i.e., it does not change significantly within the energy intervals $\sim\Gamma$ and Δ_E) and can be treated as a constant, $\Gamma(E)\simeq\Gamma_0$. In the other limiting case of a strong interaction, $\Gamma_0\gg\Delta_E$, the dependence $\Gamma(E)$ in Eq. (6) is the leading one, and the slow dependence in the denominator can be neglected. One should note that the simple expression (7) for the width $\Gamma(E)$ has to be modified in this limit; see details in [11].

The second moment Δ_E^2 of the SF can be found from the equation $\Delta_E^2=\Sigma_{f\neq 0}H_{0f}^2$. Here the summation is taken over the off-diagonal matrix elements H_{0f} that couple the initial state $|0\rangle$ with the others $|f\rangle$. For the TBRI model the analytical expression for Δ_E has been obtained in [8],

$$\Delta_E^2=\frac{1}{4}V_0^2 n(n-1)(m-n)(m-n+3), \tag{8}$$

where V_0^2 is the variance of the off-diagonal matrix elements of the two-body residual interaction V. In fact, for Fermi particles the width Δ_E turns out to be the same for any basis state $|0\rangle$.

Let us first start with the probability $W_0(t)$ of the system staying in the initial state. In the two limiting cases of small and very large times, the dependence W_0 is shown [18,27] to be of the following forms:

$$W_0(t)=\exp(-\Delta_E^2 t^2), \quad t\ll\frac{\Gamma_p}{\Delta_E^2} \tag{9}$$

and

$$W_0(t)=C\exp(-\Gamma_p t), \quad t\gg\frac{\Gamma_p}{\Delta_E^2}. \tag{10}$$

Here Γ_p is the imaginary part of the pole of the SF [see Eq. (6)] in the complex energy plane. In the case when the SF has the standard BW form [28,29], we have the obvious relation $\Gamma_p=\Gamma_0$ where the latter is given by the Fermi golden rule. In the other limit of a strong interaction, when the SF has the Gaussian form, the expression for Γ_p is not simple. The transition from one regime of time dependence of $W_0(t)$ to the other is schematically shown in Fig. 1.

Now we estimate the probabilities $w_f=|A_f(t)|^2$ of finding the system in other basis states. For a very small time we have

$$w_f=|\langle f|e^{-iHt}|0\rangle|^2\simeq|H_{0f}|^2t^2. \tag{11}$$

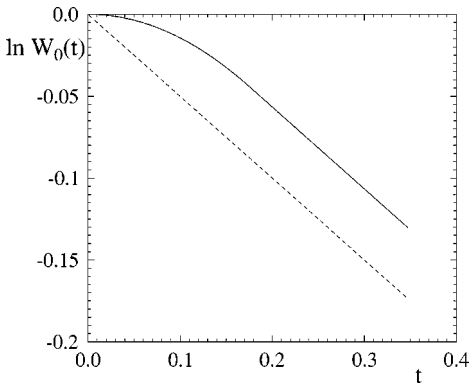

FIG. 1. Schematic time dependence of $W_0(t)$ for $\Gamma_p=0.5,\Delta_E=1.2$; the point t_c where the dependence (9) is changed to (10) is $t_c=\Gamma_p/\Delta_E^2\approx 0.17$.

Note that only the states directly connected to the initial state are populated at this time scale. One can estimate the population of these states for a larger time by substituting the time-dependent wave function $\Psi(t)=A_0(t)\psi_0+\Sigma_f A_f(t)\psi_f$ into the Schrödinger equation,

$$i\hbar\frac{dA_f}{dt}=H_{0f}(t)A_0+\sum_k H_{fk}(t)A_k. \tag{12}$$

Here $k,f\neq 0$ and $H_{0f}(t)\equiv H_{0f}\exp(i\omega_{0f}t)$. Note that the second term in the right-hand side may be treated as a random variable with zero mean value. Indeed, $A_k\propto H_{0k}$ and therefore $\overline{H_{fk}(t)H_{0f}}=0$. The variance of this term is $\Sigma_k|H_{fk}(t)A_k|^2=|H_{fk}(t)|^2\Sigma_k|A_k|^2=\overline{|H_{fk}(t)|^2}(1-|A_0|^2)$. Comparing this with the first term in the right-hand side of Eq. (12), one may conclude that the second term is not very important for small times when $A_0(t)\sim 1$. Neglecting the second term and assuming $|A_0(t)|=\exp(-\Gamma t/2)$, which is valid for $\Gamma\ll\Delta_E$, we obtain [18]

$$w_f=|H_{0f}|^2\left|\int_0^t|A_0(t)|e^{i\omega_{0f}t}dt\right|^2$$

$$\simeq\frac{|H_{0f}|^2}{\omega_{0f}^2+\Gamma^2/4}|e^{(i\omega_{0f}-\Gamma/2)t}-1|^2, \tag{13}$$

where $\omega_{0f}=E_f-E_0$. This approximate estimate shows that only the basis states within the energy interval Γ can be substantially populated (if $\Gamma>\Delta_E$, this energy interval is equal to Δ_E).

For large times, the result is different for the perturbative and chaotic regimes. In the perturbative regime the expression (13) for w_f is the final one. In the chaotic regime the asymptotic expression for $t\to\infty$ can be obtained in the following way. The projection of $\Psi(t)$ [see Eq. (3)] onto the state f gives

$$w_f(t)=w_f^s+w_f^{fluct}(t), \tag{14}$$

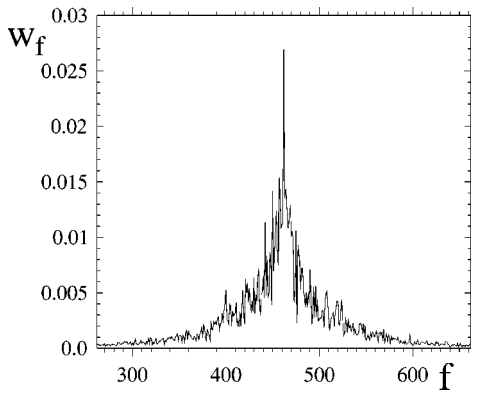

FIG. 2. Asymptotic distribution w_f for the case when the strength function is of the Breit-Wigner form in the TBRI model. The parameters are $n=6$, $m=12$, $V_0^2 \approx 0.003$, $\Gamma_0 \approx 0.50$, $\Delta_E \approx 1.16$, with the average over $N_g=10$ matrices with different realizations of random two-body matrix elements (see text).

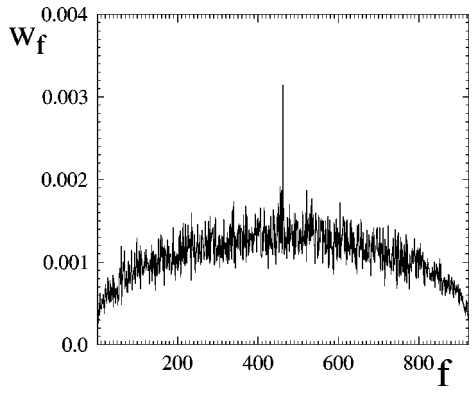

FIG. 3. Asymptotic distribution w_f for the case when the strength function is close to Gaussian. The only difference from Fig. 2 is the interaction strength $V_0^2 \approx 0.083$, and correspondingly $\Gamma_0 \approx 10.5$ and $\Delta_E \approx 5.8$; the average was taken over $N_g=50$ matrices.

$$w_f^s = \sum_k |C_0^{(k)}|^2 |C_f^{(k)}|^2 \simeq \int \frac{dE}{\rho(E)} P_0(E) P_f(E)$$

$$\simeq \frac{1}{2\pi\rho} \frac{\Gamma_t}{(E_0-E_f)^2+(\Gamma_t/2)^2}. \tag{15}$$

Here the result is written for the case when the SF has the BW form for both initial $|0\rangle$ and final states $|f\rangle$ with the corresponding FWHM's Γ_0^0 and Γ_0^f. In this case the resulting form of w_f^s is, approximately, again the Breit-Wigner with the new FWHM $\Gamma_t \simeq \Gamma_0^0 + \Gamma_0^f \simeq 2\Gamma_0$. However, if $\Gamma_0 \geqslant \Delta_E$, the form of w_f^s is close to Gaussian with the variance $(\Delta_E)_t^2 \simeq 2\Delta_E^2$ [18].

The term $w_f^{fluct}(t)$ can be written in the form

$$w_f^{fluct}(t) = \sum_{k,p;k\neq p} C_0^{(k)} C_f^{(k)} C_0^{(p)} C_f^{(p)} \exp[i(E^{(k)}-E^{(p)})t]. \tag{16}$$

At large time, $t\to\infty$, the terms in the sum rapidly oscillate and one can put $\overline{w_f^{fluct}(t)}=0$. Thus, asymptotically the distribution of the components in the time-dependent wave function is close to that given by the form of the strength function [see Eqs. (5) and (6)], with a slightly larger spreading width.

Note that the similar expression for W_0 contains the term $|C_0^{(k)}|^4$. For Gaussian fluctuations of the components $C_0^{(k)}$, one can get $\overline{|C_0^{(k)}|^4} = 3\,(\overline{|C_0^{(k)}|^2})^2$, which is the known result in random matrix theory [29,30]. Therefore, if the number of principal components N_{pc} in the SF is very large, the probability of finding the system in the initial state $|0\rangle$ at large times is at least three times larger than the probability of finding the system in any other state $|f\rangle$ (see Figs. 2 and 3).

In these figures the distribution of probabilities w_f in the TBRI model is shown after a very long time $t=40$ for two different strengths of interaction (in fact, the time t is measured in units $\hbar/d_0$ where $d_0=\langle \epsilon_{s+1}-\epsilon_s \rangle$ is the mean level spacing between single-particle energies ϵ_s). In both cases $n=6$ Fermi particles occupy $m=12$ orbitals and therefore the total number of many-particle states (the size of the Hamiltonian matrix) is $N=924$. The distribution of ϵ_s is taken random with $d_0=1$. Two-body matrix elements are taken as Gaussian random entries with zero mean and variance V_0^2, and in order to reduce the fluctuations the distribution w_f is obtained with an average over a number N_g of matrices with different random realizations. Initially, only one basis state $n_0=462$ was populated at the center of the energy spectrum, in order to avoid asymmetry of the distribution in the basis representation.

The two different values of V_0 for which the distributions w_f are obtained are chosen in such a way that in one case (see Fig. 2) the strength function has the Breit-Wigner form, and in the other the form is very close to Gaussian (Fig. 3). We should recall that the above two forms occur in the energy representation, but the results are shown in the basis representation. These two representations are related through the density of states which is known to be of the Gaussian form for large numbers of particles and orbitals [6,29,30].

One can see that in both cases, Figs. 2 and 3, the probability of staying in the original basis state is much larger than in the nearest ones. Compared with the result of standard random matrix theory, one can say that there is a noticeable difference (namely, the enhancement factor in Fig. 3 is about 2.3, instead of 3.0).

III. THE CASCADE MODEL

One important question is how the entropy of quantum isolated systems increases in time at the transition to equilibrium. It is natural to define the entropy of a many-body state through the Shannon entropy,

$$S(t) = -\sum_f w_f \ln w_f = -W_0 \ln W_0 - \sum_{f\neq 0} w_f \ln w_f. \tag{17}$$

Here $W_0(t)=|A_0(t)|^2$ is the probability for the system to be in the initial state, and $w_f(t)=|A_f(t)|^2$ is the probability to

be in the basis state $|f\rangle$. In what follows we assume that the initial conditions are $W_0(0)=1$ and $w_f(0)=0$, and therefore the entropy is equal to zero for $t=0$.

In order to study the evolution of a many-particle system with two-body interaction, it is convenient to introduce subclasses for all basis states in the following way. The *first class* contains those N_1 basis states that are directly coupled with an initial state by the two-body interaction given by matrix elements H_{0f} of the interaction. Correspondingly, the *second class* consists of N_2 basis states that are coupled with the initial one in the second order of the perturbation; this coupling is determined by $H_{0\alpha}H_{\alpha f}$, etc.

Let us first consider the evolution for a large time $t \gg \Gamma/(\Delta E)^2$ (below we assume the BW shape of the SF). For this case the probabilities of the states in different classes can be determined by the ''probability conservation equations''

$$\frac{dW_0}{dt}=-\Gamma W_0,$$

$$\frac{dW_1}{dt}=\Gamma W_0-\Gamma W_1,$$

$$\cdots$$

$$\frac{dW_k}{dt}=\Gamma W_{k-1}-\Gamma W_k, \tag{18}$$

$$\cdots.$$

Here W_k is the probability for the systems to be in the class k. The first term ΓW_{k-1} in the right-hand side of Eq. (18) is responsible for the flux from the previous class, and the second term ΓW_k describes the decay of the states in the class k into the next class $k+1$. We assume that the probability of the return to the previous class can be neglected. This is a valid approximation if the number of states N_{k+1} in the next class is large in comparison with N_k of the previous class. This approach can be compared with those based on the Caley tree model [13] where the flow from each state goes into M other states; therefore, $N_k \simeq M^k$ with $M \gg 1$. Note that here we consider a system that is far from equilibrium. Indeed, if the system is in equilibrium, the probabilities for all states within the energy shell defined by the relation $|E_f-E_0| \leqslant \Gamma$ are of the same order $w_f \simeq N_{pc}^{-1}$, with N_{pc} as the total number of states inside the energy shell. Therefore, in order to neglect the return flux, one needs the condition $w_f=W_k/N_k \gg 1/N_{pc}$ to be fulfilled.

Equations (18) have the simple solution

$$W_0=\exp(-\Gamma t),$$

$$W_n=\frac{(\Gamma t)^n}{n!}\exp(-\Gamma t)=\frac{(\Gamma t)^n}{n!}W_0. \tag{19}$$

The maximal probability $W_n=(n^n/n!)\exp(-n)\approx 1/\sqrt{2\pi n}$ to be in the class n determined by the condition $dW_n/dt=0$ occurs for $t=n/\Gamma$; therefore, this solution (19) can be considered as a *cascade* in the population of different classes. Indeed, at small times $t \ll \tau \equiv 1/\Gamma$ the system is essentially in the initial state, at times $t \approx \tau$ the flow spreads into the first class, for $t=n\tau$ it spreads into the nth class, etc. For an infinite chain one can easily check the normalization condition

$$\sum_{n=0}^{\infty} W_n = \exp(-\Gamma t)\sum_{n=0}^{\infty}\frac{(\Gamma t)^n}{n!}=1. \tag{20}$$

IV. TIME DEPENDENCE OF THE ENTROPY

The above expressions allow us to find the time dependence of the entropy,

$$S(t) \approx -\sum_{n=0}^{\infty} W_n \ln\frac{W_n}{N_n}$$

$$=\Gamma t \ln M+\Gamma t-e^{-\Gamma t}\sum_{n=0}^{\infty}\frac{(\Gamma t)^n}{n!}\ln\frac{(\Gamma t)^n}{n!}, \tag{21}$$

where $w_f \approx W_n/N_n$ stands for the population of basis states of the class n with N_n as the number of states in this class [in fact, for $t \sim n\tau$ one needs to count only the states inside the energy shell since the population of the states outside the energy interval with $|E_f-E_0|>\Gamma$ is small; see Eq.(13)]. Here we have used the relations $N_n=M^n$ and $\Sigma_{n=0}^{\infty}[(\Gamma t)^n/n!]n=\Gamma t \exp(\Gamma t)$. The two last terms in the right-hand side of Eq. (21) turn out to be smaller than the first one, so one can write

$$S(t) \approx \Gamma t \ln M[1+f(t)] \tag{22}$$

with some function $f(t) \ll 1$ that slowly depends on time.

In this estimate for the increase of entropy, we did not take into account the influence of fluctuations of w_f. One can show that, for Gaussian fluctuations of the coefficients A_f with the variance given by their mean-square values, for a large number of principal components $N_{pc}(t) \equiv \exp[S(t)]$ the entropy should be corrected by a small factor of the order of $\ln 2$ (see, for example, [31]).

If one neglects the second term in Eq. (22), we obtain a linear increase of the entropy, which means that the number of principal components $N_{pc}(t)$ increases exponentially fast with time. This behavior can be compared with the linear increase of dynamical entropy $S_{cl}(t)$ in classical chaotic systems where $S_{cl}(t)$ was found to be related to exponential divergence of close trajectories in the phase space [$S_{cl}(t) \propto \lambda t$ with λ as the Lyapunov exponent; see, for example, [32]]. The nontrivial point is that the linear increase of entropy also occurs for systems without the classical limit; see the recent paper [33].

Note that for a small time the function $W_0(t)$ has the form $W_0(t)=\exp(-\Delta_E^2 t^2)$ [see Eq. (9)], not the exponential dependence $\exp(-\Gamma t)$. Therefore, one should modify the expression for the entropy in order to make it valid for small times. For this, we replace Γt in Eq. (19) by a more accurate

expression, $-\ln(W_0)$, which gives $\Delta_E^2 t^2$ for small times $t \ll \Gamma/\Delta_E^2$ and Γt for large times $t \gg \Gamma/\Delta_E^2$; therefore,

$$W_n = \frac{(\ln W_0^{-1})^n}{n!} W_0 . \tag{23}$$

It is easy to check that the normalization condition is fulfilled again,

$$\sum_{n=1}^{\infty} W_n = \sum_{n=1}^{\infty} \frac{(\ln W_0^{-1})^n}{n!} W_0 = W_0 \exp[\ln(W_0^{-1})] = 1. \tag{24}$$

For the entropy one obtains

$$S = -\sum_{n=1}^{\infty} W_n \ln\left(\frac{W_n}{N_n}\right). \tag{25}$$

At small times $t \ll \Gamma/\Delta_E^2$ the entropy is given by two terms $n=0$ and $n=1$ (direct transitions); therefore,

$$S(t) = -W_0(t)\ln W_0(t) - W_1(t)\ln\left(\frac{W_1}{N_1}\right)$$
$$\approx \Delta_E^2 t^2 \left[1 + \ln\left(\frac{\Delta_E^2 t^2}{N_1}\right)^{-1}\right]. \tag{26}$$

This expression can be compared with the direct calculation based on the relation $w_f = |H_{0f}t|^2$,

$$S(t) = \Delta_E^2 t^2 + t^2 \sum_f |H_{0f}|^2 \ln\left(\frac{1}{H_{0f}^2 t^2}\right). \tag{27}$$

There is agreement between Eqs. (26) and (27) since $\Delta_E^2 = \Sigma_f |H_{0f}|^2 = N_1 \overline{H_{0f}^2}$.

Let us now discuss the whole time dependence of the entropy, including large times t when the system is close to equilibrium. In a finite system of particles any basis state can be reached, starting from an initial state, in several "interaction steps" $(H_{0\alpha}H_{\alpha\beta}H_{\beta\gamma}\cdots)$. For example, in a system of $n=6$ particles three steps are needed since the two-body interaction cannot move more than two particles from one basis state to another. If the number of classes n_c is finite, the states in the last class do not decay [there is no term $-\Gamma W_{n_c}$ in the last equation in (18)], and the probability of being in the last class is determined from the normalization condition $W_{n_c} = 1 - \Sigma_{k=0}^{n_c-1} W_k$. The additional condition is that the considered basis states should be inside the energy interval $|E_f - E_0| \leqslant \min(\Gamma, \Delta E)$, thus limiting the number N_n of the basis states in each class. Note that the value of W_n is restricted from below by the equilibrium relation $W_n \geqslant N_n/N_{pc}$. These limitations make an "exact" expression for the entropy very complicated. Instead, we can propose the following simple expression which is approximately valid in systems with a small number of classes ($n_c \sim 1$):

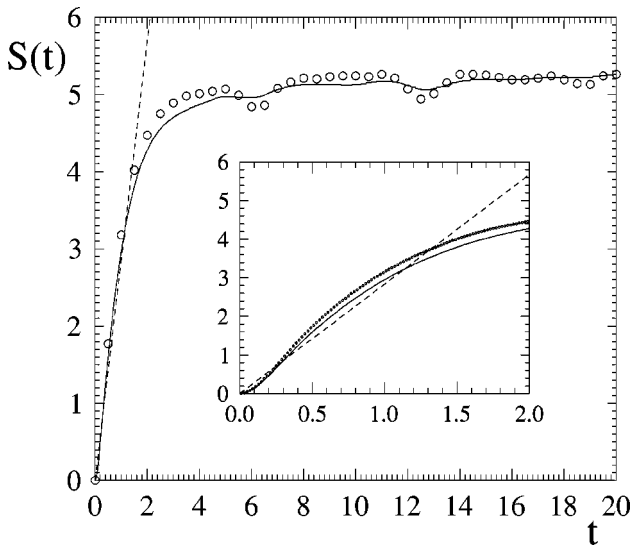

FIG. 4. Entropy versus time for the TBRI model in the case when the SF has the standard Breit-Wigner form. The parameters are the same as in Fig. 2, with $N_g = 2$. The circles stand for numerical data, the solid curve is the analytical expression (28), and the dashed line represents a linear slope according to the approximate expression (30). In the inset the same is shown for a smaller time scale.

$$S(t) = -W_0(t)\ln W_0(t) - [1 - W_0(t)]\ln\left(\frac{[1 - W_0(t)]}{N_{pc}}\right). \tag{28}$$

This expression takes into account the normalization condition $\Sigma_{f\neq 0} w_f = 1 - W_0$ and has a reasonable behavior for both small and large times.

V. NUMERICAL RESULTS FOR THE ENTROPY

Now we compare the analytical expressions obtained with numerical data for the TBRI model. For the case when the strength function has the Breit-Wigner form, the time dependence of the entropy is shown in Fig. 4 for the parameters of Fig. 2, $n=6$, $m=12$, $V_0^2 \approx 0.003$, $\Gamma_0 \approx 0.50$, $\Delta_E \approx 1.16$, with the average over $N_g = 2$ Hamiltonian matrices.

The number M of basis states directly coupled by the random two-body interaction is determined by the expression [7]

$$M = n(m-n) + \frac{n(n-1)(m-n)(m-n-1)}{4}, \tag{29}$$

where the first term gives the number of one-particle transitions, and the second stands for two-particle transitions. In our case of $n=6$ particles and $m=12$ orbitals, the total number of basis states is $N=924$ and $M=261$. The *effective number* of classes in the cascade model can be determined from the relation $M^{n_c} = N$. This gives $n_c = \ln N/\ln M \approx 1.2$. Thus, we can use the simple expression (28) to describe the dependence of the entropy on time analytically. The data in Figs. 4 and 5 demonstrate excellent agreement between the numerical and analytical results.

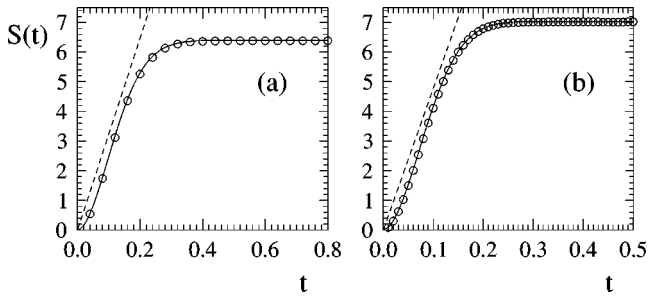

FIG. 5. Time dependence of the entropy for the TBRI model when the strength function is of the Gaussian form: (a) $n=6, m=12, V_0 \approx 0.083, \Gamma_0 \approx 10.5, \Delta_E \approx 5.8$, and (b) $n=7, m=13, V_0 \approx 0.12, \Gamma_0 \approx 14.6, \Delta_E \approx 8.13$. Circles are numerical data for $N_g=2$, solid curves stand for the approximate expression (28), and dashed lines represent the linear dependence (31).

We should note that the theoretical dependence (28) which gives a quite good approximate description of the data on the whole time scale, has a parameter N_{pc} [effective number of principal components in the stationary distribution $w_f(t\to\infty)$] that is related to the limiting value of the entropy $N_{pc}=\ln S(\infty)$. It can be estimated analytically as discussed above from the width of the energy shell; when plotting the solid curves in Figs. 4 and 5 we have used the exact value found numerically.

To avoid confusion, we should explain that the *actual number* of classes in the case of $n=6$ particles and $m=12$ orbitals is equal to 3 since all basis states can be populated in the third order in the two-body interaction. However, the number of states in the second, $k=2$, and third, $k=3$, classes is much smaller than follows from the exponential relation $N_k=M^k$ (in practice, this relation may be justified for a large number of particles only). This is the reason why the one-class formula (28) works so well.

It is also instructive to compare the entropy with the linear time dependence

$$S(t)=\Gamma t \ln M \tag{30}$$

that stems from Eq. (22) if the first term only is taken. This dependence corresponds globally to the data on some time scale; however, the actual dependence of $S(t)$ clearly differs from the linear one (see inset in Fig. 4). Note that the quadratic increase of energy occurs on a very small time scale only. As for the oscillations of the entropy for a very large time close to equilibrium, this phenomenon will be discussed below.

For a strong interaction, when the form of the SF is very close to Gaussian, numerical data are reported in Fig. 5 for $n=6$, $m=12$ and for $n=7$, $m=13$. The interaction strength is chosen in order to have the same ratio $\Gamma_0/\Delta_E \approx 1.8$ as in Fig. 4.

In this case the FWHM of the strength function is determined by Δ_E since $\Gamma_0=2\pi\rho_f H_{0f}^2$ is larger than Δ_E. As a result, Γ in the expressions (22) and (28) plays the role of the width Δ_E. In both cases numerical data give strong evidence of a linear increase of the entropy

$$S(t)=\Delta_E t \ln M \tag{31}$$

before saturation. It is clearly seen that this analytical estimate gives a correct value for the slope of $S(t)$. The shift is due to the initial time scale where the time dependence is quadratic; this fact is neglected in the estimate.

It should be pointed out that the linear dependence of $S(t)$ in Fig. 5 is much more pronounced than in the BW region (compare with Fig. 4 for which the SF is of the Breit-Wigner form). Our results indicate a clear difference between the two cases related to the Breit-Wigner and Gaussian forms of the SF. This point is supported by recent studies [23,24] where it was shown that, for a relatively weak interaction (Γ_0 is small in comparison with Δ_E) resulting in the Breit-Wigner form of the SF, there is no detailed quantum-classical correspondence for the evolution of wave packets in the energy space. On the other hand, in the Gaussian region (with the Gaussian form for the SF), a detailed quantum-classical correspondence is possible [23,24]. In the latter case one can expect a linear growth for the entropy, as was found in classical models [32]. The principal difference between these two cases (concerning the quantum-classical correspondence and the possibility of localization in the energy shell) was discussed in Ref. [21].

VI. WIDTH OF PACKETS AND INVERSE PARTICIPATION RATIO

The width of the wave function in the basis representation can be measured through the variance,

$$\Delta^2(t)=\sum_f (n_f-n_0)^2|A_f(t)|^2=[1-W_0(t)]|\Delta_f(t)|^2,$$

$$|\Delta_f(t)|^2=\frac{\sum_f (n_0-n_f)^2|A_f(t)|^2}{\sum_f |A_f(t)|^2}, \tag{32}$$

where n_f and n_0 label corresponding basis states, $f\neq 0$, and we have used the normalization condition $\Sigma_f|A_f(t)|^2=1-W_0(t)$. The function $|\Delta_f(t)|^2$ is a slow function of time; it changes from the effective bandwidth of the Hamiltonian matrix, entirely determined by the matrix elements H_{0f}, to the final width of the wave packet in the basis representation, which is defined by the width of the energy shell (approximately equal to $\sqrt{2}\Delta E$). Therefore, the leading time dependence is given by the term $1-W_0(t)$.

For relatively small times before saturation, we can use the simple estimate $w_f \approx |H_{0f}t|^2$, which results in the following quadratic dependence:

$$\Delta^2(t)\approx t^2\sum_f (n_f-n_0)^2 H_{0f}^2=t^2V_0^2\Delta_0^2. \tag{33}$$

Here Δ_0 is some constant related to the effective bandwidth of the Hamiltonian matrix. The linear dependence of the

width of the packet, $\Delta(t)=tV_0\Delta_0$, corresponds to the generic ballisticlike behavior of wave packets found for the WBRM model [23].

Note that the bandwidth of the Hamiltonian matrix can be much larger than the final width of the wave packet due to the dependence of the latter on the interaction strength. Therefore, the linear increase of $\Delta(t)$ can be very fast, and it quickly becomes saturated on the time scale of the applicability of the expansion in Ht; see Eq. (33).

Before comparing the expressions obtained with numerical data, let us first analyze the time dependence of the number of principal components $N_{pc}(t)$ for wave packets in the basis representation. It is natural to define N_{pc} through the entropy, $N_{pc}(t)=\exp[S(t)]$. This definition has been widely used in different applications; see, for example, [31].

The number of principal components can also be defined through the inverse participation ratio l_{ipr}:

$$(l_{ipr})^{-1}=\sum |A_f|^4\approx\sum_k \frac{W_k^2}{N_k}$$

$$\approx W_0^2\sum_k \frac{(\ln W_0^{-1})^{2k}}{k!k!N_k}. \tag{34}$$

Here we used Eq. (23) for W_k. The sum in Eq. (34) gives the following result for the infinite number of classes (this may be a reasonable approximation for time $t\ll n_c\tau$):

$$[l_{ipr}(t)]^{-1}=W_0^2 I_0\left(\frac{2\ln(W_0^{-1})}{\sqrt{M}}\right), \tag{35}$$

where $I_0(z)$ stands for the modified Bessel function and we used the relation $N_n=M^n$.

This expression has the following asymptotics:

$$[l_{ipr}(t)]^{-1}=W_0^2\left(1+\frac{1}{N_1}(\ln W_0^{-1})^2\right)$$

$$\approx 1-2t^2(\Delta E)^2\left(1+\frac{1}{N_1}\right) \tag{36}$$

for small time, and

$$[l_{ipr}(t)]^{-1}=\exp\left[-2\Gamma\left(1-\frac{1}{\sqrt{M}}\right)t\right] \tag{37}$$

for large time. Therefore, N_{pc} defined through the inverse participation ratio l_{ipr} may also have an interval of exponential increase in time [if the number of classes n_c is not small and we can extend the summation over k in Eq. (34) to infinity]. Here we again neglected the fluctuations of $A_f(t)$ which may increase the value of l_{ipr}^{-1} by up to a factor of 3.

For a system with a small number of classes one can suggest the approximate expression

$$[l_{ipr}(t)]^{-1}=W_0^2+\frac{(1-W_0)^2}{l_{ipr}(\infty)}. \tag{38}$$

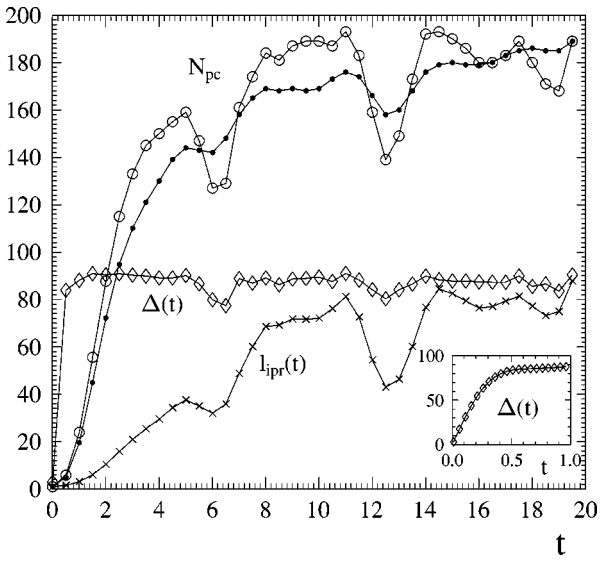

FIG. 6. Time dependence of different quantities for the TBRI model in the case of the BW form of the strength functions. The parameters are the same as in Fig. 4, with $N_g=2$. Circles stand for numerical data for $N_{pc}=\exp[S(t)]$ with $S(t)$ taken from Fig. 4, dots correspond to the analytical expression for $N_{pc}(t)$ with $S(t)$ from Eq. (28), triangles represent numerical data for the width $\Delta(t)$, and squares are numerical results for $l_{ipr}(t)$. The width $\Delta(t)$ on a smaller time scale is shown in the inset.

This expression takes into account the normalization condition $\Sigma_{f\neq 0}w_f=1-W_0$ and has a reasonable behavior for both small and large times.

In any system with a finite number of particles the energy shell contains a finite number of basis states. For a stationary chaotic state the number of principal components is estimated as $N_{pc}^{st}\sim\Gamma/D$ where D is the mean energy distance between many-particle levels (we assume here that the spreading width Γ of exact eigenstates is less than Δ_E). In the nonstationary problem this leads to the saturation of $N_{pc}(t)$ to the value $N_{pc}(\infty)\simeq 2N_{pc}^{st}$, and to the maximal value $S\approx\ln N_{pc}(\infty)$ for the entropy (see above and in Ref. [18]).

Numerical data for the TBRI model for the case when the SF is of the Breit-Wigner form are summarized in Fig. 6 for the same parameters as in Fig. 2 and Fig. 4. Three quantities are plotted here: the width $\Delta(t)$, the number of principal components $N_{pc}(t)=\exp[S(t)]$, and $l_{ipr}(t)=[\Sigma|A_f(t)|^4]^{-1}$ determined by the inverse participation ratio. For $N_{pc}(t)$ two curves are given; one is due to the analytical expression (28) for the entropy, and the other is computed directly from the evolution of the TBRI model, with an additional average over $N_g=2$ number of realizations of the random Hamiltonian.

From the reported data one can see that the time dependence of the width $\Delta(t)$ of the packets is quite simple, namely, on the first very short time scale the increase of the width is linear in time [see also the inset in Fig. 6 where $\Delta(t)$ is shown on this time scale], and afterward the width quickly saturates. This behavior is in correspondence with the analytical estimates discussed above, and with numerical results found in the WBRM [23].

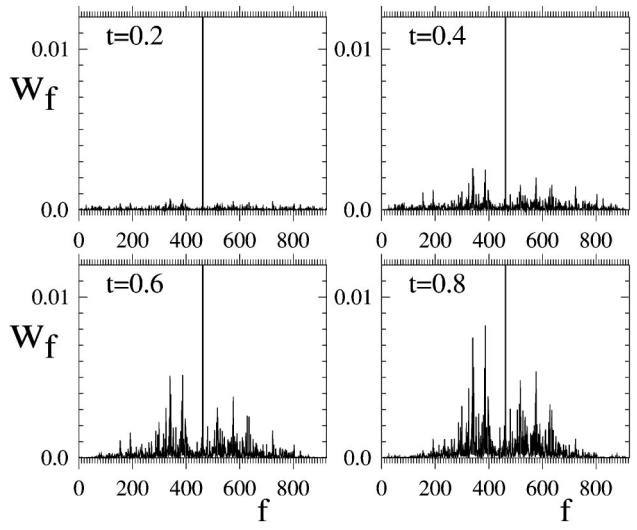

FIG. 7. Wave packet $w_f(t)$ for the TBRI model at different times $t=0.2$, 0.4, 0.6, 0.8 for the parameters of Fig. 6. One particular Hamiltonian matrix is used without any additional average.

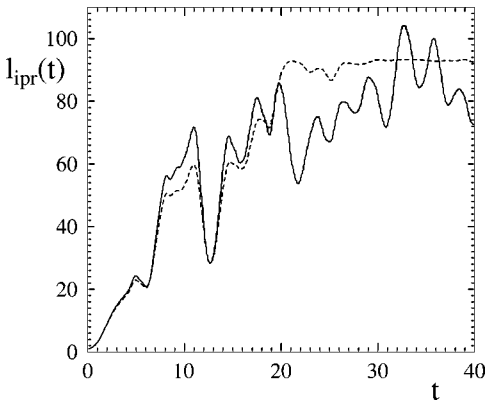

FIG. 8. Time dependence of $l_{ipr}(t)$ for the parameters of Fig. 6 on a larger time scale for one Hamiltonian matrix. The solid curve stands for numerical data, and the dashed curve corresponds to the analytical expression (38).

In contrast to this time dependence, the increase of the number of principal components $N_{pc}(t)$ is very different, both for $N_{pc}(t)$ defined by the entropy and for $l_{ipr}(t)$ determined by the inverse participation ratio. Indeed, both $N_{pc}(t)$ and $l_{ipr}(t)$ increase slowly in time before saturation to their limiting values. The absolute difference between these two quantities is not important since the definition of l_{ipr} is given up to some factor that is sensitive to the type of fluctuations in $A_f(t)$. As we already noted, the Gaussian fluctuations decrease the value of l_{ipr} by the factor 3.

One of the most interesting facts that can be drawn from these data is the big difference for characteristic time scales that correspond to saturation. Indeed, if the width $\Delta(t)$ completely saturates at time $t\approx 0.5$, both N_{pc} and l_{ipr} manifest a very slow saturation by the time $t\approx 20$. This means that the mechanism for the width increase is different from that responsible for the increase of the number of principal components in the wave packet.

To explain this phenomenon let us consider the initial time scale for the time dependence of N_{pc} and l_{ipr}, where one can detect an approximate linear increase of the entropy $S(t)$. The very point is that at small times $t\leqslant\tau$ the wave function has a large number of holes since only directly connected basis states are populated. For a system with a large number n of particles the fraction of these states is exponentially small $[\sim \exp(-n)]$ due to the two-body nature of the interaction. With increase of time, for $t\geqslant\tau=\Gamma_0^{-1}$, the states in other classes start to be filled and the holes begin to disappear. This stage for $t<n_c\tau$ corresponds to the exponential increase of the number of principal components and the linear increase of the entropy.

It is instructive to analyze the evolution of wave packets on the smaller time scale of the ballistic spread; see Fig. 7. These data confirm theoretical expectations according to which at small times only those basis states that belong to the first class are involved in the dynamics. Indeed, large gaps are clearly seen in the distribution of w_f, which persist during the whole time of the ballisticlike spread. These gaps reduce the number of principal components; however, they are not important for the calculation of $\Delta(t)$ [see Eq.(32)].

An important peculiarity of the wave dynamics is that initially *all* basis states of the first class are excited. One can see that for a very small time $t=0.2$ the whole available region $1<f<N$ is filled with approximately the same amplitudes $w_f=|H_{0f}t|^2$. With increase of time, the amplitudes grow and form the envelope of the packet, in accordance with Eq. (13). One should stress that the quadratic time dependence for the second moment of a packet on this short time scale occurs not due to a linear spread of the front of the wave packet, but due to a specific growth of the amplitudes of those basis states that are located inside the energy shell.

The remarkable effect is a kind of oscillation for all quantities of Fig. 6. Similar oscillations (although not so strong) are also present in the time dependence of the entropy $S(t)$ (see Fig. 4). Since the period $T\approx 6.5$ of these oscillations is much larger than the time scale $t\approx 0.5$ of the ballistic spread of wave packets, it is clear that this effect is entirely related to the dynamics in the Fock space formed by different classes. The origin of these oscillations can be explained in terms of the cascade model discussed in Sec. III. Indeed, one can expect a strong effect of a *reflection* due to the finiteness of the Fock space. The first reflection occurs for $t_0\approx n_c(\Gamma_0)^{-1}$; therefore, the period of oscillation is $T\approx 2t_0$. One can see that this estimate gives the correct result for T with $n_c\approx 1.5$. This value is close to our rough estimate $n_c\sim 1.2$ for an effective number of classes.

To compare the data for l_{ipr} defined by the inverse participation ratio with the analytical expression (38), we have plotted separately both results for a larger time scale $t\leqslant 40$ in Fig. 8. One can see that our estimate (38) gives a quite accurate description of the data on a large time scale up to $t\approx 20$. After this time, saturation occurs and all local time dependence may be treated as fluctuations around the limiting value. The data presented in this figure give strong evidence of the effectiveness of our analytical approach.

Let us now come to the case when the form of the strength function is close to Gaussian. In Fig. 9 one can see

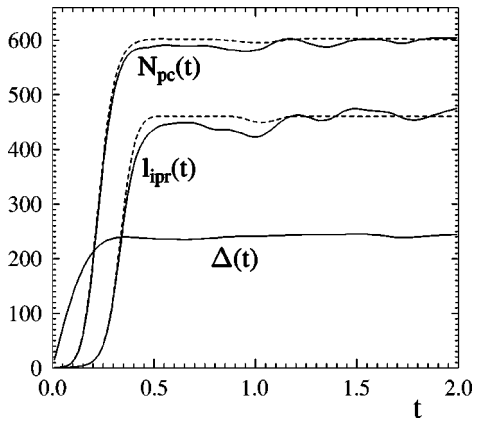

FIG. 9. The same quantities as in Fig. 6 for a strong interaction with the Gaussian form of the SF. The parameters for the TBRI model are the same as in Fig. 5(a): $n=6$, $m=12$, $V_0 \approx 0.083$, $\Gamma_0 \approx 10.5$, $\Delta_E \approx 5.8$. Solid curves correspond to numerical data, dashed curves stand for the corresponding analytical expressions Eq. (38) for $l_{ipr}(t)$ and Eq. (28) for $S(t)$ in the definition $N_{pc}(t) = \exp[S(t)]$.

that the analytical expressions connecting the probability $W_0(t)$ of staying in an initial basis state with the time dependence of the number of principal components $N_{pc}(t) = \exp[S(t)]$ and $l_{ipr}(t)$ give a correct global description of the numerical data. When compared with the previous case of the BW form of the SF (see Figs. 6 and 8) one can conclude that for a strong interaction (when the Gaussian dependence for the SF emerges) the behavior of all quantities does not reveal strong oscillations. This effect is related to the fact that the time scale for the saturation of the width of packets is of the same order as that for the saturation of both N_{pc} and l_{ipr}. In such a case the effect of reflection in the Fock space is suppressed by the strong spread of packets in the energy shell.

One can see, that there is a quite strong difference in the time dependence of all quantities discussed above for the two extreme cases of the Breit-Wigner and Gaussian forms of the strength function. In the BW case the two effects (ballistic-like spread of packets and cascadelike evolution in Fock space) have very different time scales, and both these effects can be distinguished in the dynamics. Contrarily, in the second case of the Gaussian form of the SF, the two time scales are comparable. Therefore, the two effects coexist on the same time scale and, as a result, the global time dependence turns out to be much simpler.

VII. COMPARISON WITH WIGNER BAND RANDOM MATRICES

In this section we discuss numerical results obtained for the WBRM model for the same quantities as considered above. The dynamics of wave packets in this model has been studied recently in [23] in connection with the problem of quantum-classical correspondence. Here, instead, we concentrate our attention on the correspondence between the evolution of packets in the WBR and TBRI models.

As was mentioned, the WBR model is quite close to the TBRI model. It consists of two parts, one of which is a diagonal matrix with increasing "energies" ϵ_j and the other a band matrix V_{ij},

$$H_{ij} = \epsilon_j \delta_{ij} + V_{ij}, \tag{39}$$

where δ_{ij} is the delta function. In the original papers [20] the "unperturbed spectrum" was taken in the form of the "picket fence," $\epsilon_j = jD$, where $D = \rho_0^{-1}$ is the spacing between two close energies and j is a running integer number. We consider here the case with random values ϵ_j with mean spacing D, reordered in an increasing way $\epsilon_{j+1} > \epsilon_j$. As for the off-diagonal matrix elements V_{ij}, they are assumed to be Gaussian, random, and independent variables inside the band $|i-j| \leqslant b$, with the zero mean $\langle V_{ij} = 0 \rangle$ and variance $\langle V_{ij}^2 \rangle = V_0^2$. Outside the band, the matrix elements vanish. Thus, the control parameters of this model are the ratio V_0/D of a typical matrix element to the mean level spacing, and the band width b. As one can see, the first term in Eq. (39) corresponds to a "mean field" H_0, and the interaction V has a finite energy range.

The SF for the WBRM was analyzed in Ref. [20]. It was analytically found that the form of the strength function essentially depends on one parameter $q = \rho_0^2 V_0^2 / b$ only. Wigner proved [20] that for a relatively strong perturbation $V_0 \gg D$ in the limit $q \ll 1$ the form of the LDOS is Lorentzian,

$$W_{BW}(\tilde{E}) = \frac{1}{2\pi} \frac{\Gamma_{BW}}{\tilde{E}^2 + \frac{1}{4}\Gamma_{BW}^2}, \quad \tilde{E} = E - Dj, \tag{40}$$

which nowadays is known as the Breit-Wigner dependence. Here the energy $\tilde{E}$ refers to the center of the distribution. The FWHM Γ_{BW} of the distribution (40) is given by the Fermi golden rule,

$$\Gamma_{BW} = 2\pi \rho_0 V_0^2. \tag{41}$$

In the other limit $q \gg 1$ the influence of the unperturbed part H_0 can be neglected and the shape of the SF tends to the shape of the density of states of the band random matrix V, which is known to be a semicircle.

Recently, Wigner's results have been extended in [22] to matrices H with the general form of V, when the variance of the off-diagonal matrix elements decreases smoothly with the distance $r = |i-j|$ from the principal diagonal. In this case the effective band size b is defined by the second moment of the envelope function $f(r)$. Another important generalization of the WBRM studied in [22] is an additional sparsity of the matrix V, which may mimic realistic Hamiltonians. In such a form, the WBRM is closer to the TBRI model; however, in the latter the sparsity of the interaction is due to the two-body nature of the interaction. As a result, the positions of zero elements are not completely random as in the WBRM; see details in [7,9].

Random matrix models of the type (39) are very useful for understanding the generic properties of the SF. The condition for the SF to be of the BW form in the WBRM has the simple form [22]

$$D \ll \Gamma_{BW} \ll \Delta_b, \quad \Delta_b = bD. \tag{42}$$

The left part of this relation indicates the nonperturbative character of the interaction, according to which many unperturbed basis states are strongly coupled by the interaction. On the other hand, the interaction should not be very strong, namely, the width Γ_{BW} determined by Eq. (41) has to be less than the width Δ_b of the interaction in the energy representation. The latter condition is generic for systems with finite range of the interaction V. One should stress that, strictly speaking, the BW form (40) is not correct since its second moment diverges. As was shown in [20,1], outside the energy range $|\tilde{E}| > \Delta_b$ the SF in the model (39) decreases with increasing energy faster than as a pure exponent.

Note, that in the TBRI model the energy scale Δ_b is irrelevant since there is no sharp border of the interaction and Δ_b is of the order of the whole energy spectrum. For this reason, instead of Δ_b it is more convenient to use the variance Δ_E^2 of the SF, which may have the classical limit [21,23]. The latter quantity can be expressed through the off-diagonal matrix elements of the interaction, $\Delta_E^2 = \Sigma_j V_{ij}^2$ for $i \neq j$, and therefore $\Delta_E^2 = 2bV_0^2$. As a result, we have $\Delta_b = \pi \Delta_E^2 / \Gamma_{BW}$ and Eq. (42) can be written as

$$D \ll \Gamma_{BW} \ll \Delta_E \sqrt{\pi}. \tag{43}$$

Numerical data [28] for the WBRM show that on the border $\Gamma_{BW} \approx 2\Delta_E$ the form of the SF is quite close to Gaussian, and this transition from the BW to Gaussian-like dependence turns out to be quite sharp. Although the extreme limit of a very strong interaction, $q \gg 1$ (or, the same, $\Gamma_{BW} \gg \Delta_E$), was studied by Wigner in the WBRM (39), the semicircle form of the SF seems to be unphysical. Indeed, this form originates from the semicircular dependence of the total density $\rho_V(E)$ defined by V only; i.e., when neglecting the term H_0. Thus, the case $V \gg H_0$ in terms of the TBRI model means that the residual interaction is much stronger than the mean-field part H_0, which is physically irrelevant.

Numerical data for the WBRM in the case of the BW dependence of the SF are given in Fig. 10. When compared with the corresponding quantities discussed above for the TBRI model (see Fig. 6) we should note the following. First of all, one can see that the simple analytical expression (28) gives a correct description of the increase and saturation of the entropy $S(t)$. We can say the same about the expression (38) for the number of principal components defined through the inverse participation ratio.

Second, we would like to stress that the global time dependence for all quantities is quite similar to that found for the one-class variant of the TBRI model. The relatively simple structure of the Wigner band random matrices allows one to perform a detailed comparison of the data with analytical estimates. Indeed, the application of the relation (33) for the WBRM model gives

$$\Delta^2(t) = \frac{2}{3} t^2 V_0^2 b^3, \tag{44}$$

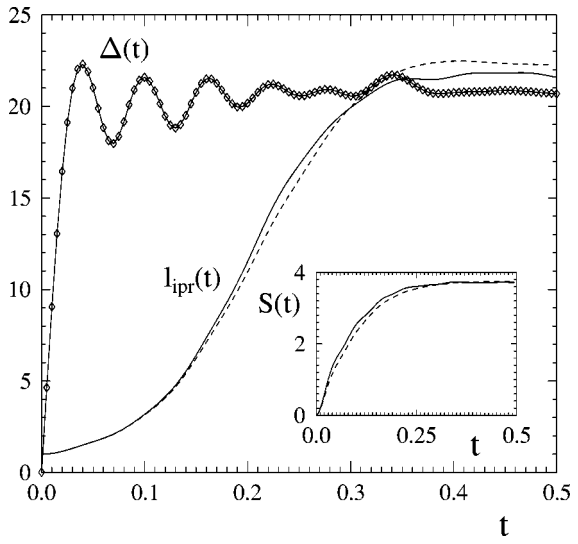

FIG. 10. Time dependence of the entropy $S(t)$ (in the inset), the width of the packet $\Delta(t)$, and the number of principal components $l_{ipr}(t)$ for the WBRM for the case of the BW form of the SF. The parameters are $N=924$, $b=110$, $D=1.0$, $V_0=1.0$, and correspondingly $\Gamma_{BW} \approx 6.28$, $\Delta_E \approx 14.8$. Solid curves for $S(t)$ and $l_{ipr}(t)$ are numerical data, dashed curves represent analytical expressions (28) [for $S(t)$] and (38) (for l_{ipr}). Diamonds, connected by the solid line, correspond to numerical data for $\Delta(t)$.

see also Ref. [19]. Therefore, for the parameters of Fig. 10 we have $\Delta(t) = Bt$ with $B = \sqrt{\frac{2}{3}} b^{3/2} V_0 \approx 950$, which is in good agreement with numerical data. We can also find the critical time t_d after which the ballistic spread of the packet terminates. For this, we estimate the maximal width Δ_m of packet via the width Δ_E of the SF, $\Delta_m \approx \sqrt{2}\Delta_E$. This leads to the estimate $t_m \approx \sqrt{6}/b$, and therefore for Fig. 3 we have $t_m \approx 21$, which corresponds perfectly to the data. These estimates have also been checked for other values of V_0 and b, with the same good correspondence between simple estimates and numerical data.

Comparing the global time dependence of the quantities presented in Fig.10 with the results for the TBRI model (see Fig. 6), one can see that the main difference is the type of oscillations for the width of packets $\Delta(t)$. That is, in contrast to the TBRI model where the period of oscillation is much larger than the time scale t_m of the ballistic spread, in Fig. 10 the period T is just defined by the ballistic spread, $T \approx 2t_m$. This very fact demonstrates the principal difference between the two models.

Indeed, for the WBRM there is no specific evolution in the Fock space due to the two-body nature of the interaction. Formally, the cascade model can be applied to the WBRM with the number of classes $n_c = 1$, since all states within the energy band $\Delta_b = bD$ start to be involved in the dynamics immediately. This means that, in contrast to the TBRI model, in the WBRM there is only one mechanism for the oscillations, namely, the reflection inside the energy shell that is populated *ergodically*, when time is running. No oscillations are detected for the number of principal components (the data for larger times are not shown); this confirms our conclusion about one kind of reflection from the edges of the

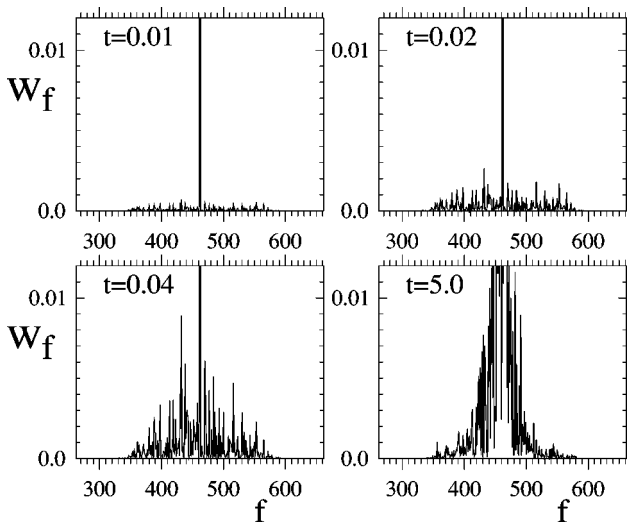

FIG. 11. Wave packet $W_n(t)$ for the WBRM at different times $t=0.01$, 0.02, 0.04, 5.0 for the parameters of Fig. 10. One particular band random matrix is used without any additional average.

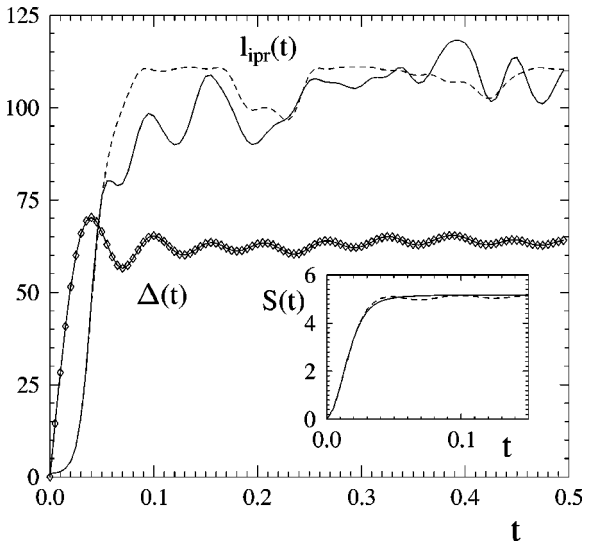

FIG. 12. The same as in Fig. 10 for the case when the form of the SF is close to Gaussian. The parameters are $N=924$, $b=110$, $D=1.0$, $V_0=3.0$, and correspondingly $\Gamma_{BW}\approx 56.5$, $\Delta_E\approx 45.5$.

energy shell. It is interesting to note that the number of principal components does not reveal noticeable oscillations on the time scale of the ballistic spread since on this scale the value of N_{pc} is very small.

The difference between these two models can also be seen when comparing the structure of wave packets in the basis representation at some time instants before the saturation (compare Fig. 11 with Fig. 7). In contrast to Fig. 7 where many ''holes'' can be realized in the distribution w_f, for the WBRM the filling of the available energy range of size $2bD$ occurs ergodically. In both cases very strong fluctuations are present, which are expected to be Gaussian (see discussion in [8]). It is important to stress that in order to reveal this difference we should avoid the ensemble average which washes out the presence of holes (if different Hamiltonian matrices have different unperturbed spectra). This fact reflects one of the basic peculiarities of the TBRI, namely, the nonergodic character of the matrices [the average over the spectrum inside one (very big) matrix may give a completely different result from that obtained by an ensemble average; see references in the review [30])].

Finally, we present the data for the WBRM in the case of the Gaussian form of the strength function (see Fig. 12). Here we can also see oscillations in the width of packets. As for the number of principal components found from the inverse participation ratio, numerical data manifest the oscillations, as well, with the same period as for the width of packets. In average, the numerical data for $S(t)$ and l_{ipr} are well described by the simple analytical expressions relating these quantities to the probability $W_0(t)$ of staying in the initial state.

The most interesting result that can be drawn from the numerical data presented in Fig. 10 and Fig. 12 is a clear difference in the time dependence of the entropy $S(t)$. Comparing the data in the insets, one can conclude that a linear increase of the entropy occurs for the case when the form of the SF is close to Gaussian, but not for the case of the BW form. Indeed, it is hard to indicate a clear time scale of the linear increase of $S(t)$ in Fig. 10, in contrast to Fig. 12 where the linear time dependence is clearly seen (apart from the very small time scale). This very fact may be quite generic, since in the TBRI model we also see a nonlinear character of the entropy increase in the BW regime.

VIII. CONCLUSIONS

In conclusion, we have studied the evolution of closed Fermi systems by making use of the standard model with random two-body matrix elements. Our main interest is in the dynamics of packets in the unperturbed energy representation, for the case when initially only one basis state is excited. The problem of the spread of the energy due to the interaction between particles is important in many physical situations, such as complex atoms and nuclei, metallic clusters, and spin systems.

First, we briefly discussed the simpler question of the probability $W_0(t)$ of finding the system in an initial state. As is known, the time dependence of this quantity is entirely determined by the spreading function which is also known in solid state physics as the local density of states. Typically, this function is assumed to be of the Lorentzian form (L regime); however, in our two-body random interaction model it depends on the interaction strength, and for a relatively strong interaction between particles it is close to Gaussian (G regime). This situation was found to be typical in complex nuclei [3] where the residual pseudorandom interaction is quite strong.

In order to analyze the dynamics of our model for any interaction strength, we suggest a phenomenological expression for the SF that interpolates between the Lorentzian and Gaussian and depends on a few control parameters of the model. This expression allows one to find the time dependence $W_0(t)$ in both the L and G regimes (see details in [27]; one should also note that the problem of a long-time

asymptotic for decay of a single-particle state was recently considered in [34]).

It is a much more difficult problem to find global characteristics for the evolution of wave packets. For this, one needs to know the time dependence for all probabilities $W_f(t)$. To treat this problem analytically, we suggest a simple cascade model that describes the dynamics of excitation in the Fock space of the system. This model is based on the fact that any given basis state interacts not with all basis states but with those that are directly coupled by a two-body interaction. As a result, it is more convenient to describe the excitation in terms of subclasses that are defined by the two-body interaction.

The cascade model allows us to find an analytical solution for $W_f(t)$ for a large number of particles, by neglecting the reverse energy flow. Using the expressions obtained, we have studied some important quantities that characterize the global dynamics of the wave function.

First we analyzed how the entropy $S(t)$ of the system increases due to the spread of packets in the unperturbed basis. For this, we used the standard definition of the Shannon entropy of wave packets, expressed by Eq. (17). Although the entropy $S(t)$ depends on the basis, it gives important information about wave packets (which also depend on the chosen basis). Indeed, this entropy can be used to find the effective number $N_{pc} \sim \exp[S(t)]$ of principal components presented in the wave packet. It should be pointed out that the Shannon entropy of stationary eigenstates in some cases may be directly related to the thermodynamical entropy (which is known to be basis independent); see, e.g., [35] and references therein.

For small times the increase of entropy in our model was found to have quadratic time dependence, $S(t) \sim t^2$, which seems to be generic. The most interesting question is about the time dependence of $S(t)$ on the large time scale before the saturation of wave packets. One of the most interesting results we found is that the increase of $S(t)$ turns out to be different depending on the form of the strength function. It was found that in the G regime the entropy increases linearly in time on a large time scale. The simple analytical estimate of $S(t)$ obtained from the cascade model agrees perfectly with direct numerical computations.

It is important to note that the linear increase of $S(t)$ was recently revealed in classical dynamical systems with chaotic behavior [32]. The rate of entropy increase was numerically found to be defined by the Lyapunov exponent that characterizes the exponential divergence of close trajectories in the phase space. Note that our model has no classical limit. In this respect, it is very interesting to understand whether there is any connection between these two facts.

Analogously, we have studied the time dependence of the width of wave packets, determined via the second moment, and the inverse participation ratio, which is widely used for the estimate of N_{pc}. Our analytical expressions give good agreement with numerical data, in spite of the relatively small number $(n=6)$ of particles. This means that the simple cascade model gives an adequate description of the evolution of wave packets in the unperturbed basis of many-particle states.

The numerical study has revealed a quite interesting phenomenon of periodic oscillations for all quantities discussed above. We showed that these oscillations are due to the finite number of classes in the cascade model, which is a consequence of the finite size of the Fock space. Simple estimates based on the cascade model with finite Fock space give the correct value for the period of these oscillations. It is interesting to note that in the basis representation these oscillations are reflected by a periodic change of the sparsity of wave packets and may be observed in real physical systems.

Finally, we performed numerical experiments with the so-called Wigner band random matrices which have been studied recently in great detail in connection with chaotic conservative Hamiltonian systems [19,21–24]. Comparison with the two-body interaction model has shown to what extent the dynamics of the wave packets is similar.

ACKNOWLEDGMENTS

This work was supported by the Australian Research Council. One of us (F.M.I.) gratefully acknowledges support by CONACyT (Mexico), Grant No. 34668-E.

[1] V. V. Flambaum, A. A. Gribakina, G. F. Gribakin, and M. G. Kozlov, Phys. Rev. A **50**, 267 (1994).

[2] G. F. Gribakin, A. A. Gribakina, and V. V. Flambaum. Aust. J. Phys. **52**, 443 (1999).

[3] M. Horoi, V. Zelevinsky, and B. A. Brown, Phys. Rev. Lett. **74**, 5194 (1995); V. Zelevinsky, M. Horoi, and B. A. Brown, Phys. Lett. B **350**, 141 (1995); N. Frazier, B. A. Brown, and V. Zelevinsky, Phys. Rev. C **54**, 1665 (1996); V. Zelevinsky, B. A. Brown, M. Horoi, and N. Frazier, Phys. Rep. **276**, 85 (1996).

[4] V. V. Flambaum, in Proceedings of the 85th Nobel Symposium [Phys. Scr. **46**, 198 (1993)].

[5] B. Georgeot and D. L. Shepelyansky, Phys. Rev. Lett. **81**, 5129 (1998).

[6] J. B. French and S. S. M. Wong, Phys. Lett. **35B**, 5 (1970); O. Bohigas and J. Flores, *ibid.* **34B**, 261 (1971).

[7] V. V. Flambaum, G. F. Gribakin, and F. M. Izrailev, Phys. Rev. E **53**, 5729 (1996).

[8] V. V. Flambaum and F. M. Izrailev, Phys. Rev. E **56**, 5144 (1997).

[9] F. M. Izrailev, in *New Directions in Quantum Chaos*, Proceedings of the International School of Physics ''Enrico Fermi,'' Course CXLIII, Varenna, 1999, edited by G. Casati, I. Guarneri, and U. Smilansky (IOS Press, Amsterdam, 2000), pp. 371–430.

[10] T. Guhr, A. Müller-Groeling, and H. A. Weidenmüller, Phys. Rep. **200**, 189 (1999).

[11] V. V. Flambaum and F. M. Izrailev, Phys. Rev. E **61**, 2539 (2000).

[12] J. Flores, M. Horoi, M. Müller, T. H. Seligman, Phys. Rev. E **63**, 026204 (2001); T. Rupp, H. A. Weidenmüller, and J. Richert, e-print nucl-th/0003053; L. Benet and H. A. Weidenmüller,

e-print cond-mat/0005103; L. Benet, T. Rupp, and H. A. Weidenmüller, cond-mat/0010425.
[13] B. L. Altshuler, Y. Gefen, A. Kamenev, and L. S. Levitov, Phys. Rev. Lett. **78**, 2803 (1997).
[14] S. Äberg, Phys. Rev. Lett. **26**, 3119 (1990); V. V. Flambaum, F. M. Izrailev, and G. Casati, Phys. Rev. E **54**, 2136 (1996); V. V. Flambaum and F. M. Izrailev, *ibid.* **55**, R13 (1997); D. L. Shepelyansky and O. P. Sushkov, Europhys. Lett. **37**, 121 (1997); B. Georgeot and D. L. Shepelyansky, Phys. Rev. Lett. **79**, 4365 (1997); P. Jacquod and D. L. Shepelyansky, *ibid.* **79**, 1837 (1997); C. Mejia-Monasterio, J. Richert, T. Rupp, and H. A. Weidenmüller, *ibid.* **81**, 5189 (1998); P. G. Silvestrov, *ibid.* **79**, 3994 (1997); Phys. Rev. E **58**, 5629 (1998).
[15] V. V. Flambaum and O. P. Sushkov, Nucl. Phys. A **412**, 13 (1984); V. V. Flambaum and G. F. Gribakin, Prog. Part. Nucl. Phys. **35**, 423 (1995).
[16] G. E. Mitchell, J. D. Bowman, and H. A. Weidenmüller, Rev. Mod. Phys. **71**, 445 (1999).
[17] B. Georgeot and D. L. Shepelyansky, Phys. Rev. E **62**, 3504 (2000); **62**, 6366 (2000).
[18] V. V. Flambaum, Aust. J. Phys. **53**, 489 (2000); e-print quant-ph/9911061.
[19] F. M. Izrailev, T. Kottos, A. Politi, S. Ruffo, and G. Tsironis, Phys. Rev. E **55**, 4951 (1997).
[20] E. P. Wigner, Ann. Math. **62**, 548 (1955); **65**, 203 (1957).
[21] G. Casati, B. V. Chirikov, I. Guarneri, and F. M. Izrailev, Phys. Lett. A **223**, 430 (1996).
[22] Y. V. Fyodorov, O. A. Chubikalo, F. M. Izrailev, and G. Casati, Phys. Rev. Lett. **76**, 1603 (1996).
[23] D. Cohen, F. M. Izrailev, and T. Kottos, Phys. Rev. Lett. **84**, 2052 (2000).
[24] D. Cohen and T. Kottos, e-print nlin.CD/0001026; e-print cond-mat/0004022.
[25] F. M. Izrailev, in Proceedings of the Nobel Symposium ''Quantum Chaos Y2K'' [Phys. Scr., T **T90**, 95 (2001)].
[26] A. Bohr and B. Mottelson, *Nuclear Structure* (Benjamin, New York, 1969), Vol. 1.
[27] V. V. Flambaum and F. M. Izrailev, Phys. Rev. E (to be published).
[28] G. Casati, V. V. Flambaum, and F. M. Izrailev (unpublished).
[29] V. K. B. Kota and R. Sahu, Phys. Rev. E **64**, 016219 (2001).
[30] T. A. Brody, J. Flores, J. B. French, P. A. Mello, A. Pandey, and S. S. M. Wong, Rev. Mod. Phys. **53**, 385 (1981).
[31] F. M. Izrailev, Phys. Rep. **196**, 299 (1990).
[32] V. Latora and M. Baranger, Phys. Rev. Lett. **82**, 520 (1999); A. K. Pattanayak, *ibid.* **83**, 4526 (1999); M. Barranger, V. Latora, and A. Rapisarda, e-print cond-mat/0007302.
[33] P. Grigolini, M. G. Pala, and L. Palatella, Phys. Lett. A **285**, 49 (2001).
[34] P. G. Silvestrov, e-print cond-mat/0103222.
[35] P. Cejnar, V. Zelevinsky, and V. V. Sokolov, Phys. Rev. E **63**, 036127 (2001).